5. *PAPER IV*: BCHJ FUNCTIONS LIKE A MAGNESIUM-PROTOPORPHYRIN IX CARRIER BETWEEN MAGNESIUM CHELATASE AND *S*-ADENOSYL-L-METHIONINE: MAGNESIUM-PROTOPORPHYRIN IX *O*-METHYLTRANSFERASE IN *RHODOBACTER CAPSULATUS*

5.1 Synopsis

- Determined the interaction between magnesium chelatase and *O*-methyltransferase or BchJ from *Rba. capsulatus* using magnesium chelatase assays
- BchJ was heterologously expressed and purified
- Spectroscopically established that both BchJ and BchM bind proto and Mg-proto
- Upon Mg-proto binding, BchJ had a flexible secondary structure, while BchM was comparatively rigid
- BchM and BchJ shifted the reaction equilibrium of magnesium chelatase by removing Mg-proto from BchH
- A 1:1 molar ratio of BchH-Mg-proto:BchM/BchJ was found
- Interaction of BchH with BchM prevailed over BchH-BchJ suggesting BchJ is a porphyrin carrier

5.2 Manuscript

Paper IV

FEBS Journal

BchJ functions like a magnesium-protoporphyrin IX carrier between magnesium chelatase and S-adenosyl-L-methionine:magnesium-protoporphyrin IX O-methyltransferase in Rhodobacter capsulatus

Journal:	*FEBS Journal*
Manuscript ID:	Draft
Manuscript Type:	Regular Paper
Subdiscipline:	Enzymes and catalysis
Date Submitted by the Author:	
Complete List of Authors:	Sawicki, Artur; Macquarie University, Chemistry and Biomolecular Sciences Willows, Robert; Macquarie University, Chemistry and Biomolecular Sciences
Key Words:	magnesium chelatase, bacteriochlorophyll, Rhodobacter capsulatus, methyltransferase, porphyrin, heme, tetrapyrrole

Title: BchJ functions like a magnesium-protoporphyrin IX carrier between magnesium chelatase and *S*-adenosyl-L-methionine:magnesium-protoporphyrin IX *O*-methyltransferase in *Rhodobacter capsulatus*

Authors' names: Artur Sawicki and Robert D Willows

Address: Department of Chemistry and Biomolecular Sciences, Macquarie University, NSW 2109, Australia

Corresponding author: Robert D Willows, Department of Chemistry and Biomolecular Sciences Macquarie University NSW 2109 Australia, rwillows@rna.bio.mq.edu.au, Ph +6 298508146, Fax +6 298508245

Departmental website http://www.chem.mq.edu.au/

Running title: Interaction of BchM/BchJ with magnesium chelatase

Abbreviations: BchM, *S*-adenosyl-L-methionine:magnesium-protoporphyrin IX *O*-methyltransferase, DTT, dithiothreitol, Mg-proto, magnesium-protoporphyrin IX, proto, protoporphyrin IX, SAM, *S*-adenosyl-L-methionine

Keywords: Bacteriochlorophyll biosynthesis, BchJ, BchM, magnesium chelatase, *O*-methyltransferase

Subdivision: Enzymes and catalysis

Summary

Substrate channelling between the enzymatic steps in the (bacterio)chlorophyll biosynthetic pathway catalyzed by magnesium chelatase (BchI/ChlI, BchD/ChlD, and BchH/ChlH subunits) and *S*-adenosyl-L-methionine:magnesium-protoporphyrin IX *O*-methyltransferase (BchM/ChlM) has been suggested. This involves delivery of magnesium protoporphyrin IX from the BchH/ChlH subunit of magnesium chelatase to BchM/ChlM. Stimulation of BchM/ChlM activity by BchH/ChlH was previously shown, and physical interaction of the two proteins has been demonstrated. In plants and cyanobacteria there is an added layer of complexity as Gun4 serves as a porphyrin (protoporphyrin IX and magnesium-protoporphyrin IX) carrier but this protein does not exist in anoxygenic photosynthetic bacteria. Recently it was proposed that another protein, BchJ may fulfill a similar role since it has no currently assigned function in the well established pathway.

In this study we further characterized the magnesium chelatase-BchM interaction by focussing upon magnesium chelatase assays. We purified BchJ from *Rhodobacter capsulatus* and conducted experiments with this protein in parallel with BchM. Our results suggested that both BchM and BchJ interacted with the BchH-Mg-protoporphyrin IX subunit of magnesium chelatase in a 1:1 molar ratio. Despite this similarity, BchM and BchJ were differentiated in this interaction by their release or retention of magnesium-protoporphyrin IX respectively. BchM exhibited the dominant interaction with BchH-Mg-protoporphyrin IX over BchJ in a coupled magnesium chelatase assay. We propose that BchJ could play a role as a magnesium-protoporphyrin IX transporter between BchH and BchM.

Introduction

Magnesium chelatase (E.C. 6.6.1.1) and *S*-adenosyl-L-methionine:magnesium-protoporphyrin IX *O*-methyltransferase (BchM) (E.C. 2.1.1.11) catalyze sequential steps of the (bacterio)chlorophyll biosynthetic pathway [1-4]. Magnesium chelatase requires free magnesium and ATP hydrolysis to convert protoporphyrin IX (proto) to magnesium-protoporphyrin IX (Mg-proto) [5-12]. This is followed by *O*-methyltransferase using the ubiquitous methylating molecule *S*-adenosyl-L-methionine (SAM) to convert Mg-proto to Mg-proto monomethyl ester [13-16]. Magnesium chelatase is the more complex of the two enzymes, composed of at least three subunits. It consists of BchI, BchD, and BchH subunits from bacteriochlorophyll biosynthetic bacteria or ChlI, ChlD, and ChlH subunits from chlorophyll biosynthetic organisms including bacteria, algae and plants. There are differences in complexity of magnesium chelatase depending on the organism. For example *Arabidopsis thaliana* (*A. thaliana*) has two ChlI isoforms [17] with each protein contributing to magnesium chelatase activity and complex formation [18-20]. The green sulphur bacterium *Chlorobaculum tepidum* (*C. tepidum*) has the unique property of having three isoforms of BchH [21, 22], with suggestions of regulatory properties of at least one subunit [23]. BchI and BchD hexamers [24-26] form a symmetrically stacked BchID complex, with each subunit composed of a trimer of dimers or dimer of trimers [27], and BchD providing a stable platform for BchI [24]. The largest subunit of magnesium chelatase, BchH, contains proto bound [8, 28, 29] and transiently interacts with the BchID complex [30, 31]. This interplay initiates a burst of ATPase activity supplied by BchI which drives magnesium chelation to form Mg-proto [32, 33]. It has been shown in plants (*A. thaliana*) and cyanobacteria (*Synechocystis*) that a subsidiary porphyrin binding protein, Gun4 associates with ChlH and increases magnesium chelatase activity [34-37]. This interaction was recently localized at the chloroplast membranes [38] which is consistent with single protein studies of both Gun4 and ChlH existing in the stroma and membrane [35, 39, 40]. Currently there is no identified homolog of Gun4 in anoxygenic photosynthetic bacteria and it was suggested that BchJ, a protein absent in plants, algae, and most bacteria could play a similar role to Gun4 in purple (sulphur and non-sulphur) bacteria and green

sulphur bacteria [1, 41]. This was postulated since BchJ lacks 8-vinyl reductase activity [41], which contradicted the conclusions drawn from previous mutational studies of *bchJ* [42]. However the role of BchJ has not been studied so it has no classified role in bacteriochlorophyll biosynthesis.

O-methyltransferase has been thoroughly characterized biochemically in the 1970's-80's [43-46] with studies also conducted on highly purified his-tagged enzymes from *Synechocystis* [47, 48], *Rhodobacter capsulatus* (*Rba. capsulatus*) [49], and *C. tepidum* [23]. The enzyme is membrane-associated [14-16, 44, 50], and is a high-molecular weight polymer in anaerobic bacteria [23, 49], whereas the cyanobacterial form is soluble as a monomer [48]. The recent report showing the potential of a continuous coupled colorimetric assay for SAM-dependent methyltransferase enzymes [51] was validated with ChlM of *Synechocystis* yielding kinetic constants comparable to previous uncoupled HPLC-based stopped assays for *O*-methyltransferase [52]. Other work has found an inextricable link between folate biosynthesis and *O*-methyltransferase activity, which was due to the C1 pathway [53] and SAM/SAH metabolic levels [54].

The interaction between magnesium chelatase and *O*-methyltransferase has been known for over 35 years through initial experiments using whole cells of *Rba. sphaeroides* [55]. However the precise nature of the interaction was not apparent until much later particularly due to the complexity of magnesium chelatase. A breakthrough occurred with the discovery that BchH is the porphyrin binding subunit with a ~1:1 molar ratio of protein:porphyrin [8]. Since this subunit shares the ability to bind Mg-proto with *O*-methyltransferase, interactions between BchH/ChlH of magnesium chelatase and *O*-methyltransferase may be possible. Studies using *Synechocystis* showed a large stimulation of *O*-methyltransferase activity with ChlH up to ~10-fold on a millisecond time-scale [56]. A 1.3-1.6-fold increase in *O*-methyltransferase activity was also found with BchS and BchT isoforms of BchH from *C. tepidum* [23]. BchH from this species actually reduced *O*-methyltransferase activity prompting the idea it could be involved in regulation [23]. Some evidence also exists for BchH-BchM interactions in *Rba. capsulatus* [57], however crude protein preparations were used in this study and the precise molecular

interaction could not be deduced. Our previous findings showed no distinct impact of *O*-methyltransferase activity upon addition of various magnesium chelatase subunits, including the fully functional BchIDH complex [49]. Another study showed magnesium chelatase activity acted in parallel with *O*-methyltransferase activity in transgenic sense and antisense ChlM Tobacco plants [58]. The RNA and protein expression of ChlH and *O*-methyltransferase also acted in unison [58]. Another report showed the physical interaction between ChlH and ChlM from Tobacco with a yeast 2-hybrid system [59].

In this study we wish to present further evidence highlighting the interaction between magnesium chelatase, BchM, and BchJ from the purple non-sulphur bacterium *Rba. capsulatus*. Our results predominantly focussed upon the shift in magnesium chelatase reaction equilibria of proto/Mg-proto upon addition of BchM or BchJ. We provide kinetic evidence of a direct interaction between BchM or BchJ with the BchH-Mg-proto subunit of magnesium chelatase, and show a concentration-dependent effect. Our data also suggested there is an interaction between BchM and BchJ. We propose that BchJ may serve as an Mg-proto carrier between BchH-Mg-proto and BchM.

Results and Discussion

Physical and structural properties of BchJ

BchJ was readily purified to homogeneity in a single step using metal affinity chromatography (Fig. S1). BchJ (22 kD) behaved as a high molecular weight complex by size-exclusion chromatography even in the presence of detergent Triton X-100 (Fig. S2). It has already been shown that BchM exists as a large molecular weight multimer in both purple non-sulfur and green sulphur bacteria by gel filtration [23, 49] and this is different to ChlM from *Synechocystis* which exists as a monomer [48].

Our CD spectroscopy data showed BchM and BchJ have well-defined and similar secondary structure compositions, with the majority of secondary structure being alpha-helical (52-53 %). There is a relatively large proportion of unordered structure (19/25 %) for BchJ/BchM, and BchJ has a higher proportion of beta strands over BchM alone (20.8/9.1 %) (Fig. 1 and Table S1).

Effect of magnesium upon BchM or BchJ, and their interactions with magnesium chelatase

Since coupled magnesium chelatase assays with BchM or BchJ requires free magnesium, we first tested if magnesium would be detrimental to BchM or BchJ individually in terms of solubility. Free magnesium above ~2 mM caused substantial aggregation of BchM, whereas BchJ was mildy affected at ~8 mM (Fig. 2A). In terms of their effect on magnesium chelatase, BchM, BchJ, or detergent Tween 80 all increased product formation of magnesium chelatase in a similar manner at concentrations above 2 mM free magnesium. BchM also showed this effect at lower free magnesium concentrations tested (0.78 and 1.2 mM) (Fig. 2B). The aggregation of BchM in this study could explain the adverse effect of magnesium previously observed in *O*-methyltransferase activity (65 % reduction at 10 mM) [49]. Interactions of BchM, BchJ, or Tween 80 with magnesium chelatase suggested magnesium chelatase first has to form a stable complex before it can effectively interact with BchJ or Tween 80, whereas BchM may participate in the stabilization of the magnesium chelatase complex. The interaction of BchM or BchJ with magnesium chelatase is comparable at higher magnesium concentrations (Fig. 2B) which indicated the aggregative effect of magnesium had no negative impact on the ability of BchM to interact with magnesium chelatase. This implied that BchM may naturally act as an aggregate.

Using the aggregation of BchM or BchJ to co-precipitate magnesium chelatase subunits

We further analyzed interactions of magnesium chelatase with BchM or BchJ by looking at the distribution of proteins into soluble and insoluble fractions. It should be noted that the supernatant fractions (Fig. 3A) had one sixth of the relative loading of the pellet fractions (Fig. 3B). At the magnesium concentration used, BchH was largely soluble, BchM was largely insoluble, whereas BchJ existed in both the soluble and insoluble fractions (Fig. 3A and B). Addition of BchM or BchJ to magnesium chelatase significantly increased the proportion of BchH into the insoluble fraction. There was a less distinct increase in BchI and BchD into the insoluble fraction, thus suggesting there is a

physical interaction between BchH and BchM or BchH and BchJ. The interaction involved aggregates of each protein indicating a membranous interaction may occur *in vivo*.

Spectroscopic analysis of BchM or BchJ with Mg-proto and proto; soret and far-UV changes

BchH can bind proto and Mg-proto [8, 28, 29] so we tested the ability of BchM or BchJ to bind proto and Mg-proto because this may provide more information on BchM/BchJ-BchH interactions. Both BchM and BchJ could bind proto and Mg-proto *in vitro* using absorbance spectroscopy (Fig. 4). Soret spectra of BchM and BchJ were red-shifted by ~10 and 25 nm for Mg-proto and proto respectively with positive (Tween 80) and negative (aldolase) controls for comparison. Thus the absorbance spectra indicated BchM or BchJ change the environment of proto/Mg-proto similar to micellar Tween 80, implying a specific binding of the porphyrins to a hydrophobic pocket. The shift in soret is characteristic of a non-planar rearrangement of the porphyrins [60]. Distortion of the tetrapyrrole nucleus is common in nature (reviewed by Shelnutt et al.) [60], most notably seen with many heme (iron tetrapyrrole) binding proteins, but also nickel porphyrin binding protein (cofactor F_{430}), and bacteriochlorophyll binding photosynthetic reaction centres.

We further tested soret and far-UV properties of BchM and BchJ, and when bound to Mg-proto using CD (Fig. 1). BchM showed changes in the soret region upon binding Mg-proto but there was no obvious change in the far-UV region (Fig. 1 and Table S1). The differences in the soret region upon Mg-proto binding to BchM signifies asymmetric changes in porphyrin planarity. Therefore it is suggested that BchM has a rigid secondary structure that undergoes relatively little change upon binding Mg-proto, instead causing Mg-proto distortion. An even more prominent shift in the soret CD signal was previously observed using apomyoglobin reconstituted with hemin [61]. Contrastingly BchJ showed no structural changes upon binding Mg-proto in the soret region, however significant differences were observed in the CD spectra of the far-UV region. The changes in the far-UV region were seemingly inversely related, with a decrease in beta strands (20.8 to 6.2 %) balanced by an increase in regular alpha helices (34 to 47

%) (Table S1). Thus, in comparison to BchM, BchJ showed a comparatively malleable secondary structure with the changes presumably needed to accommodate Mg-proto since the porphyrin largely retained its conformation. This tentatively suggested that BchJ may potentially bind other similar porphyrins as shown recently with Gun4 [38].

Interaction between magnesium chelatase and BchM, BchJ, or Tween 80

Previous findings have consistently shown the BchH subunit of magnesium chelatase enhances *O*-methyltransferase activity with *C. tepidum*, *Synechocystis*, *Rba. capsulatus* and Tobacco [23, 56, 57, 59, 62], and thus it was implied that *O*-methyltransferase accepts the Mg-proto substrate when bound to BchH. We found that BchM could utilize Mg-proto produced *in situ* from BchH with Mg-proto monomethyl ester made in the complete coupled assay (BchIDHM SAM) (Fig. S3). Since Mg-proto is retained by BchH following catalysis [29], this conclusively shows that BchM directly uses BchH-Mg-proto as a substrate as previously suggested using *Synechocystis* [62]. We wished to more accurately quantify the respective interactions of BchM, BchJ, or Tween 80 with BchH. Our experiments here focussed on the magnesium chelatase assay because our previous findings could not establish a unique stimulatory effect of magnesium chelatase subunits upon *O*-methyltransferase activity [49]. We initially found that BchM, BchJ, or Tween 80 generated an increased amount of Mg-proto produced by magnesium chelatase over time (Fig. 5). The time taken to reach equilibrium was significantly faster for BchM over BchJ and Tween 80. This suggested that BchM was the primary interacting partner with BchH compared with BchJ and Tween 80. Our subsequent experiments concentrated on the total amount of product made by magnesium chelatase in the presence of BchM, BchJ, or Tween 80 additives at equilibrium. Detailed kinetic analysis revealed that the nature of BchM and BchJ interactions with BchH was different when compared with Tween 80 (Fig. 6). Namely the effect of each protein is ratio-dependent with respect to BchH-proto concentration, while Tween 80 showed a concentration-dependent effect that was independent of BchH-proto concentration. Thus the apparent K_m of BchM and BchJ increased in parallel with ascending BchH-proto concentrations, whereas a global K_m was determined

with Tween 80 (3.6 ± 0.2 μM). This was deemed the best analysis of Tween 80 since plotting individual K_m values only generated a range of 2.1-5.4 μM. The slope of apparent K_m versus BchH-proto concentration for BchM and BchJ respectively was 0.51 ± 0.06 and 0.54 ± 0.03 (Fig. 6D), indicating both BchM and BchJ have a 1:1 molar interaction with BchH. The optimal effect of Tween 80 is nearing the critical micelle concentration (CMC) (10 μM) [63], thus suggesting that micellar formation is important. The Tween 80 micellar molecular mass is ~78,600 as inferred from the aggregation number [64] and the recently determined cylindrical/discus-shaped structure of Tween 80 by small-angle X-ray scattering [65] is suggested to be important for sequestering Mg-proto from BchH. Optimal amounts of either BchM, BchJ, or Tween 80 enabled magnesium chelatase to completely convert all of the proto bound to BchH into Mg-proto, compared with 71 % conversion without these additives (Fig. 7). Our results showed that either BchM, BchJ, or Tween 80 can shift the equilibrium of the magnesium chelatase reaction to the product side by removing or sequestering Mg-proto from BchH.

Location of Mg-proto when equilibrium is shifted

Once equilibria of magnesium chelatase with BchM or BchJ was attained, each protein behaved differently in terms of interaction with Mg-proto. We tested BchM with and without SAM, which produced either Mg-proto monomethyl ester or Mg-proto respectively. BchM had the characteristic ability to release Mg-proto or Mg-proto monomethyl ester from BchH into the soluble fraction, whereas BchJ remained associated with Mg-proto and BchH in the insoluble fraction (Fig. 8). When BchM and BchJ were combined with magnesium chelatase, BchM had the dominant effect over BchJ (Mg-proto was released), which supported the time course experiment (Fig. 5). These results suggested there may be an interaction between BchM and BchJ involving the transfer of Mg-proto. It is proposed that partly soluble BchJ is a likely candidate for transfer of Mg-proto between the soluble BchH protein and membranous BchM.

Conclusions

In this study we compared and contrasted the interaction of BchM or BchJ with magnesium chelatase. Kinetic data suggested the interaction of either BchM or BchJ involved a 1:1 molar ratio with BchH-Mg-proto of magnesium chelatase, despite severe aggregation of BchM. BchM could directly interact with BchH-Mg-proto and hand off Mg-proto or Mg-proto monomethyl ester in the absence or presence of SAM respectively. BchJ acted as a magnesium-porphyrin binding protein that can remove Mg-proto from BchH, and we suggest that BchJ probably delivers Mg-proto to BchM for catalysis.

Experimental procedures

Cloning of BchJ

The plasmid pRPS404 consisting of the *Rba. capsulatus* photosynthetic gene cluster [66] was used as the template in the 5 PRIME PCR extender system using the following primers; For 5'-CAGCCATATGCTCGAGATGAGCGGTGCCGCGCCT-3' and Rev 5'-CAGCCGGATCCTCGAGTCAGCCGGAGTGGACAGA-3'. The PCR method was as follows; initial denaturation at 94 ºC for 2 min, followed by 30 cycles consisting of a denaturing step at 94 ºC for 30 s, annealing at 65 ºC for 30 s, and extension at 72 ºC for 40 s. There was a final extension period of 2 min at 72 ºC. The purified PCR product (Sigma GenElute PCR Clean-Up kit) was then mixed together with pET15b vector (Invitrogen) previously digested using XhoI (Fermentas). Cloning and transformation was performed according to the In Fusion 2.0 dry-down PCR cloning kit (Clontech). Transformants were analyzed by colony PCR and positive clones were sequenced using the T7 forward primer 5'-TAATACGACTCACTATAGGG-3' (Invitrogen). The pET15bBchJ construct was subcloned into BL21(DE3) Star *E. coli* for expression and protein purification.

Expression and protein purification

Expression and purification of magnesium chelatase subunits (BchI, BchD, and BchH) and *O*-methyltransferase (BchM) was performed as previously described [10, 32], and [49] respectively. Protein expression and purification of 6x-his-tagged BchJ was achieved according to BchM with the following

modifications. Harvested cells were resuspended in 125 mM imidazole, lysed (French Press at 700 bar) and the supernatant was directly applied to a 5-mL HisTrap Ni^{2+} crude FF chelating column (GE Healthcare Biosciences). The column was washed with 50 column volumes of the same buffer, followed by elution with 20 mM Tris-HCl pH 7.9, 500 mM NaCl and 500 mM imidazole. Fractions containing eluted protein were pooled, desalted and concentrated with repeated washing using 5 mM Tricine-NaOH pH 8.0, and 1.1 M glycerol (10 kDa cut-off centrifugation device, Millipore). Typical yields were approximately 0.5-1 mg protein from 2 L culture. Concentrated protein was centrifuged twice at 18,000 *g* for 5 min at room temperature before aliquots of the supernatant were snap frozen and stored at -80 °C.

Protein determination

Protein determinations for BchI, BchD, BchJ, and BchM were performed using Bio-Rad protein assay reagent [67] according to the manufacturer's instructions with BSA as a standard. BchH-proto concentration was determined as previously described [32] with all assays consisting of a 1.3:1 ratio of BchH:proto.

CD spectroscopy

Measurements were carried out with a Jasco J-810 Spectrometer at 20 °C using a 10 mm path length cuvette. Wavelength scans were generated from 185–450 nm at 100 $nm.min^{-1}$, with 1 nm bandwidth, 2 s response time, and 32 accumulations.

Magnesium chelatase assays

Assays were performed at 30 °C as previously described [24, 32] with the following final concentrations unless otherwise stated in figure legends; 50 mM Tricine-NaOH pH 8.0, 12.5 mM $MgCl_2$, 2.2 mM dithiothreitol (DTT), 1 mM ATP, 0.7 mM urea, 10.5 mM glycerol (assay buffer), and 12 nM BchD, 25 nM BchI, and 150 nM BchH-proto. Concentrations of Mg-proto made were determined at equilibrium whereupon the rate of magnesium chelatase was below 0.05 ± 0.03 nmol $Mg\text{-}proto.min^{-1}.nmol^{-1}$ BchD.

Kinetic analysis

The Michaelis-Menten equation ($V= V_{max}*[S]/(K_m + [S])$) was used for nonlinear regression analysis with GraphPad Prism Version 5.01 for Windows (GraphPad Software, San Diego, CA).

Calculation of free magnesium

Concentration of magnesium in our stock magnesium chloride solutions was determined by atomic absorption spectrometry (GBC Scientific Equipment 932 AA spectrophotometer). The following instrument parameters were used; lamp current, 3.0 mA, wavelength, 285.2 nm with a magnesium lamp, slit width of 0.5 nm, time constant of 0.1, air-acetylene gas at fuel flow of 21 $L.min^{-1}$, air-flow at 10 $L.min^{-1}$, and three replicates of each reading. Magnesium standards (Choice Analytical) were prepared in 100 mL volumetric flasks in distilled water and used to construct a standard curve ($R^2= 0.991$). The actual magnesium concentrations used for our assays were determined after our stock magnesium chloride concentrations were compared with the standard curve. These values were then used in WEBMAXCLITE version 1.15 software (http://www.stanford.edu/~cpatton/MgATP-NIST.htm) [68] at ionic strength 0.05, and 30 ° C with the appropriate ATP concentrations to determine free magnesium used in the assays.

***O*-Methyltransferase assays and RP-HPLC separation of porphyrins**

Assays were performed as described previously [49] and in figure legend and stopped with addition of an equal volume of stop solution (80 % acetone). Samples were centrifuged at 18,000 *g* for 5 min, Tween 80 added to the supernatant to make a final concentration of 300 μM, and the supernatant analyzed by RP-HPLC. RP-HPLC was performed as previously described [49] with the following modifications. The HPLC method used a gradient of 0-67 % water to acetonitrile over 15.5 min at 2 $mL.min^{-1}$ with a Shimadzu RF-535 Fluorescence detector (excitation at 412 nm, and emission at 602 nm) and SPD-M20 diode array detector.

Spectrophotometry

Absorbance spectra were taken using a Beckman DU 640 spectrophotometer at 240 nm.min^{-1} with a 10 mm path length cuvette. Concentrations of BchM, BchJ, aldolase, proto and Mg-proto (where used) were all 400 nM, whereas Tween 80 was 100 μM.

Porphyrins

The preparation and handling of Mg-proto and Mg-proto monomethyl ester standards was performed as previously described [49].

References

1. Chew AGM & Bryant DA (2007b) Chlorophyll Biosynthesis in Bacteria: The Origins of Structural and Functional Diversity. *Ann Rev Microbiol* **61**, 113-129.
2. Willows RD (2003) Biosynthesis of chlorophylls from protoporphyrin IX. *Nat Prod Rep* **20**, 1-16.
3. Willows RD & Kriegel AM (2009) Biosynthesis of Bacteriochlorophyll in Purple Bacteria. In *The Purple Phototrophic Bacteria* (Hunter CN, Daldal F, Thurnauer MC & Beatty JT, ed^eds), pp. 57-79. Springer Science, Dordrecht.
4. Beale SI & Weinstein JD (1990) Tetrapyrrole metabolism in photosynthetic organisms. In *Biosynthesis of Heme and Chlorophylls* (Dailey HA, ed^eds), pp. 287-391. McGraw-Hill Publishing, New York.
5. Jensen PE, Gibson LCD, Henningsen KW & Hunter CN (1996) Expression of the *chlI*, *chlD*, and *chlH* Genes from the Cyanobacterium *Synechocystis* PCC6803 in *Escherichia coli* and Demonstration That the Three Cognate Proteins Are Required for Magnesium-protoporphyrin Chelatase Activity. *J Biol Chem* **271**, 16662-16667.
6. Reid JD & Hunter CN (2002) Current understanding of the function of magnesium chelatase. *Biochem Soc Trans* **30**, 643-645.
7. Walker CJ & Willows RD (1997) Mechanism and regulation of Mg-chelatase. *Biochem J* **327**, 321-333.
8. Willows RD, Gibson LCD, Kanangara CG, Hunter CN & von Wettstein D (1996) Three separate proteins constitute the magnesium chelatase of *Rhodobacter sphaeroides*. *Eur J Biochem* **235**, 438-443.
9. Willows RD & Hansson M (2003) Mechanism, structure, and regulation of magnesium chelatase. In *The Porphyrin Handbook* (Kadish KM, Smith KM & Guilard R, ed^eds), pp. 1-47. Academic Press, Sydney.
10. Willows RD & Beale SI (1998) Heterologous Expression of the *Rhodobacter capsulatus BchI*, *-D*, and *-H* Genes That Encode Magnesium Chelatase Subunits and Characterization of the Reconstituted Enzyme. *J Biol Chem* **273**, 34206-34213.
11. Jensen PE, Gibson LCD & Hunter CN (1998) Determinants of catalytic activity with the use of purified I, D and H subunits of the magnesium protoporphyrin IX chelatase from *Synechocystis* PCC6803. *Biochem J* **334**, 335-344.
12. Gibson LC, Willows RD, Kannangara CG, von Wettstein D & Hunter CN (1995) Magnesium-protoporphyrin chelatase of *Rhodobacter sphaeroides*: reconstitution of activity by combining the products of the *bchH*, *-I*, and *-D* genes expressed in *Escherichia coli*. *Proc Natl Acad Sci* **92**, 1941-1944.
13. Bollivar DW (2003) Intermediate steps in chlorophyll biosynthesis:methylation and cyclization. In *The Porphyrin Handbook, Chlorophylls and bilins:biosynthesis, synthesis, and degradation* (Kadish KM, Smith, K. M., Guilard, R., ed^eds), pp. 49-69. Academic Press, Sydney.

14. Gibson KD, Neuberger A & Tait GH (1963) Studies on the biosynthesis of porphyrin and bacteriochlorophyll by *Rhodopseudomonas spheroides*. *Biochem J* **88**, 325-334.
15. Tait GH & Gibson KD (1961) The enzymic formation of magnesium protoporphyrin monomethyl ester. *Biochim Biophys Acta* **52**, 614-616.
16. Block MA, Tewari AK, Albrieux C, Maréchal E & Joyard J (2002) The plant S-adenosyl-L-methionine:Mg-protoporphyrin IX methyltransferase is located in both envelope and thylakoid chloroplast membranes. *Eur J Biochem* **269**, 240-248.
17. Rissler HM, Collakova E, DellaPenna D, Whelan J & Pogson BJ (2002) Chlorophyll biosynthesis. Expression of a second *Chl I* gene of Magnesium chelatase in Arabidopsis supports only limited chlorophyll synthesis. *Plant Physiol* **128**, 770-779.
18. Apchelimov A, Soldatova O, Ezhova T, Grimm B & Shestakov S (2007) The analysis of the ChlI 1 and ChlI 2 genes using acifluorfen-resistant mutant of *Arabidopsis thaliana*. *Planta* **225**, 935-943.
19. Kobayashi K, Mochizuki N, Yoshimura N, Motohashi K, Hisabori T & Masuda T (2008) Functional analysis of *Arabidopsis thaliana* isoforms of the Mg-chelatase *CHLI* subunit. *Photochem Photobiol Sci* **7**, 1188-1195.
20. Huang Y-S & Li H-m (2009) Arabidopsis CHLI2 Can Substitute for CHLI1. *Plant Physiol* **150**, 636-645.
21. Frigaard N-U & Bryant DA (2004) Seeing green bacteria in a new light: genomics-enabled studies of the photosynthetic apparatus in green sulfur bacteria and filamentous anoxygenic phototrophic bacteria. *Arch Microbiol* **182**, 265-276.
22. Frigaard N-U, Chew A, Li H, Maresca J & Bryant D (2003) *Chlorobium Tepidum* : Insights into the Structure, Physiology, and Metabolism of a Green Sulfur Bacterium Derived from the Complete Genome Sequence. *Photosynth Res* **78**, 93-117.
23. Johnson ET & Schmidt-Dannert C (2008) Characterization of Three Homologs of the Large Subunit of the Magnesium Chelatase from *Chlorobaculum tepidum* and Interaction with the Magnesium Protoporphyrin IX Methyltransferase. *J Biol Chem* **283**, 27776-27784.
24. Axelsson E, Lundqvist J, Sawicki A, Nilsson S, Schroder I, Al-Karadaghi S, Willows RD & Hansson M (2006) Recessiveness and Dominance in Barley Mutants Deficient in Mg-Chelatase Subunit D, an AAA Protein Involved in Chlorophyll Biosynthesis. *Plant Cell* **18**, 3606-3616.
25. Willows RD, Hansson A, Bircha D, Al-Karadaghi S & Hansson M (2004) EM single particle analysis of the ATP-dependent BchI complex of magnesium chelatase: an AAA+ hexamer. *J Struct Biol* **146**, 227-233.
26. Fodje MN, Hansson A, Hansson M, Olsen JG, Gough S, Willows RD & Al-Karadaghi S (2001) Interplay between an AAA module and an integrin I domain may regulate the function of magnesium chelatase. *J Mol Biol* **311**, 111-122.
27. Elmlund H, Lundqvist J, Al-Karadaghi S, Hansson M, Hebert H & Lindahl M (2008) A New Cryo-EM Single-Particle Ab Initio Reconstruction Method Visualizes Secondary Structure Elements in an ATP-Fueled AAA+ Motor. *J Mol Biol* **375**, 934-947.
28. Karger GA, Reid JD & Hunter CN (2001) Characterization of the Binding of Deuteroporphyrin IX to the Magnesium Chelatase H Subunit and Spectroscopic Properties of the Complex. *Biochemistry* **40**, 9291-9299.
29. Sirijovski N, Lundqvist J, Rosenback M, Elmlund H, Al-Karadaghi S, Willows RD & Hansson M (2008) Substrate-binding model of the chlorophyll biosynthetic magnesium chelatase BchH subunit. *J Biol Chem* **283**, 11652-11660.
30. Gräfe S, Saluz H-P, Grimm B & Hänel F (1999) Mg-chelatase of tobacco: The role of the subunit CHL D in the chelation step of protoporphyrin IX. *Proc Natl Acad Sci* **96**, 1941-1946.
31. Papenbrock J, Gräfe S, Kruse E, Hänel F & Grimm B (1997) Mg-chelatase of tobacco: identification of a *Chl D* cDNA sequence encoding a third subunit, analysis of the interaction of the three subunits with the yeast two-hybrid system, and reconstitution of the enzyme activity by co-expression of recombinant CHL D, CHL H and CHL I. *Plant J* **12**, 981-990.

32. Sawicki A & Willows RD (2008) Kinetic Analyses of the Magnesium Chelatase Provide Insights into the Mechanism, Structure, and Formation of the Complex. *J Biol Chem* **283**, 31294-31302.
33. Jensen PE, Gibson LCD & Hunter CN (1999a) ATPase activity associated with the magnesium-protoporphyrin IX chelatase enzyme of *Synechocystis* PCC6803: evidence for ATP hydrolysis during Mg^{2+} insertion, and the MgATP-dependent interaction of the ChlI and ChlD subunits. *Biochem J* **339**, 127-134.
34. Davison PA, Schubert HL, Reid JD, Iorg CD, Heroux A, Hill CP & Hunter CN (2005) Structural and Biochemical Characterization of Gun4 Suggests a Mechanism for Its Role in Chlorophyll Biosynthesis. *Biochemistry* **44**, 7603-7612.
35. Larkin RM, Alonso JM, Ecker JR & Chory J (2003) GUN4, a Regulator of Chlorophyll Synthesis and Intracellular Signaling. *Science* **299**, 902-906.
36. Sobotka R, Duhring U, Komenda J, Peter E, Gardian Z, Tichy M, Grimm B & Wilde A (2008) Importance of the Cyanobacterial Gun4 Protein for Chlorophyll Metabolism and Assembly of Photosynthetic Complexes. *J Biol Chem* **283**, 25794-25802.
37. Verdecia MA, Larkin RM, Ferrer J-L, Riek R, Chory J & Noel JP (2005) Structure of the Mg-Chelatase cofactor GUN4 reveals a novel hand-shaped fold for porphyrin binding. *PLoS Biol* **3**, e151.
38. Adhikari ND, Orler R, Chory J, Froehlich JE & Larkin RM (2009) Porphyrins Promote the Association of GENOMES UNCOUPLED 4 and a Mg-chelatase Subunit with Chloroplast Membranes. *J Biol Chem* **284**, 24783-24796.
39. Luo M, Weinstein JD & Walker CJ (1999) Magnesium chelatase subunit D from pea: characterization of the cDNA, heterologous expression of an enzymatically active protein and immunoassay of the native protein. *Plant Mol Biol* **41**, 721-731.
40. Nakayama M, Masuda T, Bando T, Yamagata H, Ohta H & Takamiya K-I (1998) Cloning and Expression of the Soybean *chlH* Gene Encoding a Subunit of Mg-Chelatase and Localization of the Mg^{2+} Concentration-Dependent ChlH Protein within the Chloroplast. *Plant Cell Physiol* **39**, 275-284.
41. Chew AGM & Bryant DA (2007a) Characterization of a Plant-like Protochlorophyllide a Divinyl Reductase in Green Sulfur Bacteria. *J Biol Chem* **282**, 2967-2975.
42. Suzuki JY & Bauer CE (1995) Altered Monovinyl and Divinyl Protochlorophyllide Pools in *bchJ* Mutants of *Rhodobacter capsulatus*. *J Biol Chem* **270**, 3732-3740.
43. Ellsworth RK, Dullaghan JP & St Pierre ME (1974) The reaction mechanism of S-adenosyl-L-methionine: magnesium protoporphyrin IX methyltransferase of wheat. *Photosynthetica* **8**, 375-383.
44. Hinchigeri SB, Nelson DW & Richards WR (1984) The purification and reaction mechanism of S-adenosyl-L-methionine: magnesium protoporphyrin IX methyltransferase from *Rhodopseudomonas sphaeroides*. *Photosynthetica* **18**, 168-178.
45. Hinchigeri SB & Richards WR (1982) The reaction mechanism of S-adenosyl-L-methionine:magnesium protoporphyrin IX methyltransferase from *Euglena gracilis*. *Photosynthetica* **16**, 554-560.
46. Yee WC, Eglsaer SJ & Richards WR (1989) Confirmation of a ping-pong mechanism for S-adenosyl-methionine:magnesium protoporphyrin methyltransferase of etiolated wheat by an exchange reaction. *Biochem Biophys Res Comm* **162**, 483-490.
47. Shepherd M & Hunter CN (2004) Transient kinetics of the reaction catalysed by magnesium protoporphyrin IX methyltransferase. *Biochem J* **382**, 1009-1013.
48. Shepherd M, Reid JD & Hunter CN (2003) Purification and kinetic characterization of the magnesium protoporphyrin IX methyltransferase from *Synechocystis* PCC6803. *Biochem J* **371**, 351-360.
49. Sawicki A & Willows RD (2007) S-Adenosyl-L-methionine:magnesium-protoporphyrin IX O-methyltransferase from *Rhodobacter capsulatus*: mechanistic insights and stimulation with phospholipids. *Biochem J* **406**, 469-478.
50. Averina N, Rassadina V & Leonid F (2002) Native state, energetic interaction of chlorophyll precursors and intraplastid location of S-adenosyl-L-methionine: Mg-protoporphyrin IX methyltransferase in etiolated leaves. *Ind J Exp Biol* **40**, 192-201.

51. Dorgan KM, Wooderchak WL, Wynn DP, Karschner EL, Alfaro JF, Cui Y, Zhou ZS & Hevel JM (2006) An enzyme-coupled continuous spectrophotometric assay for *S*-adenosylmethionine-dependent methyltransferases. *Anal Biochem* **350**, 249-255.
52. McLean S & Hunter CN (2009) An enzyme-coupled continuous spectrophotometric assay for magnesium protoporphyrin IX methyltransferases. *Anal Biochem* **394**, 223-228.
53. Hanson AD & Roje S (2001) One-Carbon Metabolism In Higher Plants. *Ann Rev Plant Physiol Plant Mol Biol* **52**, 119-137.
54. Van Wilder V, De Brouwer V, Loizeau K, Gambonnet B, Albrieux C, Van Der Straeten D, Lambert WE, Douce R, Block MA, Rebeille F & Ravanel S (2009) C1 metabolism and chlorophyll synthesis: the Mg-protoporphyrin IX methyltransferase activity is dependent on the folate status. *New Phytol* **182**, 137-145.
55. Gorchein A (1972) Magnesium protoporphyrin chelatase activity in *Rhodopseudomonas sphaeroides*: studies with whole cells. *Biochem J* **127**, 97-106.
56. Shepherd M, McLean S & Hunter CN (2005) Kinetic basis for linking the first two enzymes of chlorophyll biosynthesis. *FEBS J* **272**, 4532-4539.
57. Hinchigeri SB, Hundle B & Richards WR (1997) Demonstration that the BchH protein of *Rhodobacter capsulatus* activates S-adenosyl--methionine:magnesium protoporphyrin IX methyltransferase. *FEBS Lett* **407**, 337-342.
58. Alawady AE & Grimm B (2005) Tobacco Mg protoporphyrin IX methyltransferase is involved in inverse activation of Mg porphyrin and protoheme synthesis. *Plant J* **41**, 282-290.
59. Alawady A, Reski R, Yaronskaya E & Grimm B (2005) Cloning and expression of the tobacco CHLM sequence encoding Mg protoporphyrin IX methyltransferase and its interaction with Mg chelatase. *Plant Mol Biol* **57**, 679-691.
60. Shelnutt JA, Song X-Z, Ma J-G, Jia S-L, Jentzen W & Medforth CJ (1998) Nonplanar porphyrins and their significance in proteins. *Chem Soc Rev* **27**, 31-41.
61. Kawamura-Konishi Y, Kihara H & Suzuki H (1988) Reconstitution of myoglobin from apoprotein and heme, monitored by stopped-flow absorption, fluorescence and circular dichroism. *Eur J Biochem* **170**, 589-595.
62. Jensen PE, Gibson LCD, Shephard F, Smith V & Hunter CN (1999b) Introduction of a new branchpoint in tetrapyrrole biosynthesis in *Escherichia coli* by co-expression of genes encoding the chlorophyll-specific enzymes magnesium chelatase and magnesium protoporphyrin methyltransferase. *FEBS Lett* **455**, 349-354.
63. Neugebauer JM (1990) Detergents: An Overview. *Method Enzymol* **182**, 239-253.
64. de Campo L, Yaghmur A, Garti N, Leser ME, Folmer B & Glatter O (2004) Five-component food-grade microemulsions: structural characterization by SANS. *J Colloid Interface Sci* **274**, 251-267.
65. Aizawa H (2009) Morphology of polysorbate 80 (Tween 80) micelles in aqueous 1,4-dioxane solutions. *J Appl Crystallogr* **42**, 592-596.
66. Alberti M, Burke DH & Hearst JE (1995) Structure and sequence of the photosynthetic gene cluster. In *Anoxygenic photosynthetic bacteria* (Blankenship RE, Madigan MT & Bauer CE, ed^eds), pp. 1083-1106. Kluwer Academic Publishing, Amsterdam.
67. Bradford MM (1976) A rapid and sensitive method for the quantitation of microgram quantities of protein utilizing the principle of protein-dye binding. *Anal Biochem* **72**, 248-254.
68. Patton C, Thompson S & Epel D (2004) Some precautions in using chelators to buffer metals in biological solutions. *Cell Calcium* **35**, 427-431.
69. Sreerama N & Woody RW (2000) Estimation of Protein Secondary Structure from Circular Dichroism Spectra: Comparison of CONTIN, SELCON, and CDSSTR Methods with an Expanded Reference Set. *Anal Biochem* **287**, 252-260.
70. Sreerama N & Woody RW (2004) On the analysis of membrane protein circular dichroism spectra. *Protein Sci* **13**, 100-112

Acknowledgements

This work was supported by a Macquarie University Research Development Grant to R.D.W.

5.3 Supplementary data, schema and figures

Supplemental data

Fig. S1. Expression and purification of his-tagged BchJ. SDS-PAGE was performed using a 4-20 % NuSep gel. Lane M, Bio-Rad broad-range ladder with molecular weights listed on the left-hand side in kilodaltons, Lane 1. Uninduced cells, Lane 2. Induced cells, Lane 3. HisTrap purified BchJ.

Fig. S2. Approximate size determination of HisTrap purified BchM and BchJ. Size exclusion chromatography was performed with a Superose 6 10/300 column (GE Healthcare Biosciences) at a flow rate of 0.5 mL.min^{-1} with elution buffer; 10 mM Tricine-NaOH pH 8.0, 2 mM DTT, 1.3 mM $MgCl_2$, and 100 µM Triton X-100. Solid and dashed lines represent BchM and BchJ respectively. Arrow shows the void volume of the column where blue dextran (GE Healthcare Biosciences) elutes (8.02 mL). Samples of either 27 µg BchM or 90 µg BchJ prepared in elution buffer were loaded in a total volume of 100 µL.

Fig. S3. RP-HPLC separation of porphyrin products from coupled magnesium chelatase and *O*-methyltransferase assays. Each assay was performed according to magnesium chelatase experimental, with 120 nM BchH-proto, 12.5 nM BchI, 6.6 nM BchD, 21 mM glycerol, and additions of 200 µM SAM, and 0.76 µM BchM were used where present. BchIDH represents magnesium chelatase alone, BchIDH, SAM refers to magnesium chelatase with SAM, BchIDHM is magnesium chelatase with *O*-methyltransferase, and BchIDHM, SAM is magnesium chelatase with *O*-methyltransferase and SAM. Assays were stopped after 90 min, and compared to Mg-proto or Mg-proto monomethyl ester standards (bottom two traces).

Table S1. Secondary structure prediction of BchM and BchJ in the presence or absence of Mg-proto.

Predictions regarding the secondary structure of BchM and BchJ from Fig. 1 were performed with CDPro software in the range 185-250 nm using reference set SMP50 consisting of 37 soluble proteins and 13 membrane proteins [69, 70]. Composition of the secondary structures was determined using the three software programs; SELCON3, CDSSTR, and CONTINLL and their averages and standard deviations summarized in the table. H (r) refers to regular alpha helices, H (d) are distorted alpha helices, S (r) are regular strands, S (d) are distorted strands, T are turns, and U are unordered structures.

Sample	H (r)	H (d)	S (r)	S (d)	T	U
BchM	34 ± 4.5	19 ± 1.1	5.1 ± 2.7	4.0 ± 1.9	15 ± 2.7	25 ± 5.7
BchM-Mg-proto	27 ± 7.8	17 ± 3.5	7.6 ± 3.3	6.8 ± 2.2	17 ± 3.6	26 ± 6.7
BchJ	34 ± 7.7	18 ± 3.9	12 ± 8.1	8.8 ± 2.7	9 ± 7.9	19 ± 7.1
BchJ-Mg-proto	47 ± 6.8	18 ± 3.1	2.4 ± 2.9	3.8 ± 2.5	9.7 ± 6.5	20 ± 10

Schema

Schematic 1. Proposed reaction mechanism of magnesium chelatase and *O*-methyltransferase (BchM). The porphyrin substrate of magnesium chelatase is denoted as BchH-proto and the catalytic component of the enzyme is treated as the BchID complex. In the absence of BchM this reaction converts approximately 71 % of BchH-proto to BchH-Mg-proto. Upon the addition of BchM, there is a shift in the equilibria to the right, producing up to 100 % BchH-Mg-proto depending upon the concentration of BchH-proto. It appears the majority of additional Mg-proto made is released into solution in the presence of BchM at equilibrium, and in the presence of SAM, Mg-proto monomethyl ester (Mg-proto ester) is made. Interaction between magnesium chelatase and *O*-methyltransferase is a closed system with *O*-methyltransferase able to remove the Mg-proto product directly from BchH with no need for exogenous Mg-proto. An intact BchH-BchM complex is shown although it is unknown whether BchH and BchM dissociate following Mg-proto transfer to BchM.

Schematic 2. Proposed reaction mechanism of magnesium chelatase and BchJ. Magnesium chelatase together with BchJ produces up to 100 % BchH-Mg-proto, however once made, it is not readily released into solution. From our experiments it appears the majority of additional Mg-proto made remains bound to BchJ at equilibrium. At this stage it is unclear whether a BchH-BchJ-Mg-proto complex remains intact, or if BchJ-Mg-proto readily dissociates from BchH.

Figure legends

Fig. 1. Soret and far-UV **c**ircular dichroic spectra of BchM or BchJ with Mg-proto. Experiments were performed in 10 mM sodium phosphate pH 7.6, 40 µM Tricine-NaOH pH 8.0, and 8.6 mM glycerol. Concentrations of BchM, BchJ, and Mg-proto (where used) were all 400 nM. The x-axis is divided into two sections for clarity with the left hand side providing secondary structure information of the protein and right hand side depicting any interaction of protein with Mg-proto in the soret region. (A) BchM alone (open circles), or BchM together with Mg-proto (closed circles). (B) BchJ alone (open circles), or BchJ together with Mg-proto (closed circles).

Fig. 2. Aggregation of BchM or BchJ with magnesium, and their respective interactions with magnesium chelatase. All experiments contained final concentrations as described for magnesium chelatase assays except 3.2 mM DTT, 0.5 mM ATP, and variable free magnesium; 0.38, 0.78, 1.2, 2.0, 2.9, 3.7, 7.9, 12 mM were used, and where stated, 87 nM BchH-proto, 850 nM BchM/BchJ, and 64 µM Tween 80 was also included. (A) Bradford assay of BchM or BchJ with increasing magnesium concentrations. Assays were performed by adding the following components; 3.6 µL BchID buffer (assay buffer with 4.4 mM DTT, 10 mM urea, 3.5 mM glycerol), 23.8 µL MgATP (assay buffer with 4.4 mM DTT, and variable $MgCl_2$ concentrations; 0, 0.96, 1.93, 3.8, 5.8, 7.7, 17, and 27 mM), and 27.5 µL of either BchM (open circles) or BchJ (closed circles). Samples were centrifuged (18,000 *g* for 7 min at room temperature), the supernatant added to Bradford reagent (Bio-Rad) and compared to a standard curve (BSA) to generate final concentrations on the y-axis. (B) Magnesium chelatase assays with the y-axis representing the total Mg-proto produced at equilibrium. BchID (13.3 µL) was refolded in assay buffer as stated above and diluted to 100 µL with variable concentrations of MgATP, followed by addition of 100 µL BchH-proto together with either buffer alone (50 mM Tricine-NaOH pH 8.0, 19 mM glycerol, 2 mM DTT) (open squares), BchM in buffer (open circles), BchJ in buffer (closed circles), or Tween 80 in buffer (closed diamonds).

Fig. 3. Co-precipitation of magnesium chelatase subunits with BchM or BchJ; distribution of protein into soluble and insoluble fractions. M refers to Bio-Rad broad-range ladder with molecular weights in kilodaltons listed on the left-hand side. 1. BchIDH, 2. BchIDHM, 3. BchIDHJ, 4. BchIDHTween 80. Assays were performed as described for magnesium chelatase with the following final concentrations; 86 mM glycerol, 18 mM urea, 4 mM DTT, 0.33 µM BchD, 0.66 µM BchI, 1.385 µM BchH-proto, and if present, 2.7 µM BchM/BchJ, or 117 µM Tween 80 in a total volume of 160 µL. The total assay time was 90 min, followed by centrifugation at 18,000 *g* for 7 min at room temperature to separate supernatant and pellet fractions. A total volume of 25 µL supernatant was loaded onto a 4-15 % polyacrylamide gel (Bio-Rad) (A). The pellet fraction was further washed two times with 100 µL assay buffer without protein or detergent, vortexed for 10 s, and centrifuged after each wash step with the supernatant of each wash discarded. The final pellet was resuspended in 25 µL SDS-PAGE load buffer (Nu-Sep) and the total volume loaded onto the gel (B). The approximate position of each protein is listed on the right-hand side.

Fig. 4. Soret absorbance spectra showing binding of proto/Mg-proto to BchM or BchJ. All experiments were performed in 10 mM sodium phosphate pH 7.6, 40 µM Tricine-NaOH pH 8.0, and 8.6 mM glycerol. Dashed lines represent proto or Mg-proto alone, whereas filled lines show BchM, BchJ, Tween 80, or aldolase together with proto or Mg-proto. Left-hand column (A-D) represents addition of Mg-proto to BchM, BchJ, Tween 80, and aldolase respectively. Right-hand column (E-H) represents addition of proto to BchM, BchJ, Tween 80, and aldolase respectively.

Fig. 5. Product (Mg-proto) formation by magnesium chelatase increases with BchM, BchJ, or Tween 80. All magnesium chelatase assays were performed as described in experimental except 0.5 mM ATP, and 140 nM BchH-proto was used. Four assays were conducted; magnesium chelatase alone (open circles), and together with 860 nM BchM (closed circles, maroon), 860 nM BchJ (closed squares, blue), or 61 µM Tween 80 (closed triangles, orange).

Fig. 6. Differences in magnesium chelatase interactions with BchM, BchJ, or Tween 80. Magnesium chelatase assays were performed as described with final concentrations of 4 mM DTT, 330 mM glycerol 0.7 mM urea, 7.7 nM BchD, and 15.8 nM BchI. The following fixed BchH-proto concentrations were used; 3.7 nM (open circles), 7.5 nM (open squares), 15 nM (open triangles), 30 nM (open diamonds), 60 nM (closed circles), 120 nM (closed squares), and 240 nM (closed triangles). The amount of Mg-proto made at equilibrium by magnesium chelatase alone was assigned zero percent stimulation whereas one hundred percent stimulation refers to the largest total Mg-proto made with magnesium chelatase coupled with BchM, BchJ, or Tween 80. (A-C) represent variable concentrations of BchM, BchJ, and Tween 80 repectively at the fixed BchH-proto concentrations. A global apparent K_m value for (C) was determined using shared V_{max} and K_m values. (D) Apparent K_m values were determined from (A and B) at the fixed BchH-proto concentrations with open and closed circles representing BchM and BchJ respectively.

Fig. 7. Quantifying the shift in equilibrium of magnesium chelatase with BchM, BchJ, or Tween 80. Magnesium chelatase assays from Fig. 6 were re-analyzed showing the total amount of Mg-proto made by magnesium chelatase at equilibrium. Pre-determined optimal amounts of BchM, BchJ, or Tween 80 were taken from Fig. 6. Open circles represent the magnesium chelatase assay alone at the specified BchH-proto concentrations and closed circles represent the addition of BchM (A), BchJ (B), and Tween 80 (C) to the assay.

Fig. 8. Distribution of magnesium porphyrin into soluble and insoluble fractions following the shift in equilibrium by magnesium chelatase-BchM/BchJ interactions. Magnesium chelatase assays were performed as for Fig. 3 with the following modifications; 31 mM glycerol, 0.83 mM urea, 4 mM DTT, 15 nM BchD, 30 nM BchI, 342 nM BchH-proto, and if present, 150 µM SAM, 750 nM BchM/BchJ, or 117 µM Tween 80 in a total volume of 160 µL. Following centrifugation, 45 µL of supernatant was added to 155 µL of 52 % acetone and 0.013 % ammonia, centrifuged again, and this was labelled as the supernatant (s). The pellet fraction (p) was washed three times as described above. The third wash supernatant was used for correcting the final pellet fluorescence values. The final pellet was resuspended

in 710 µL 40 % acetone, 0.01 % ammonia, centrifuged and this supernatant used for fluorescence measurements.

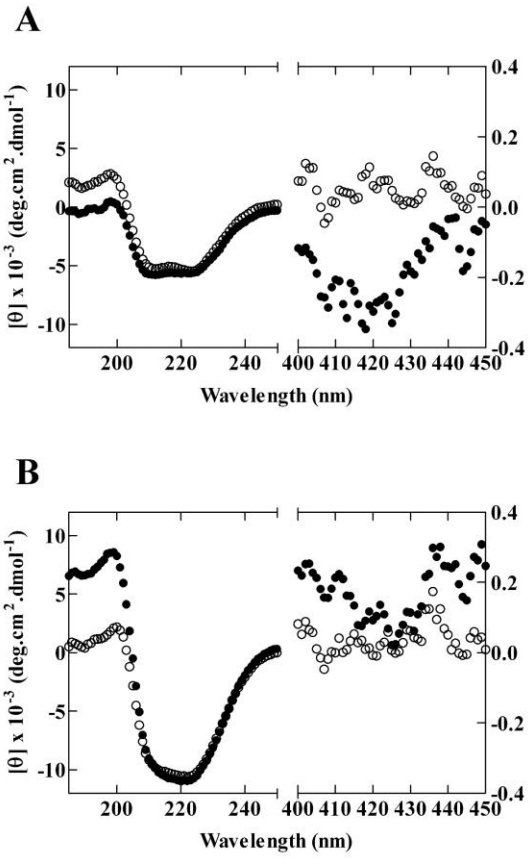

Figure 1
120x182mm (600 x 600 DPI)

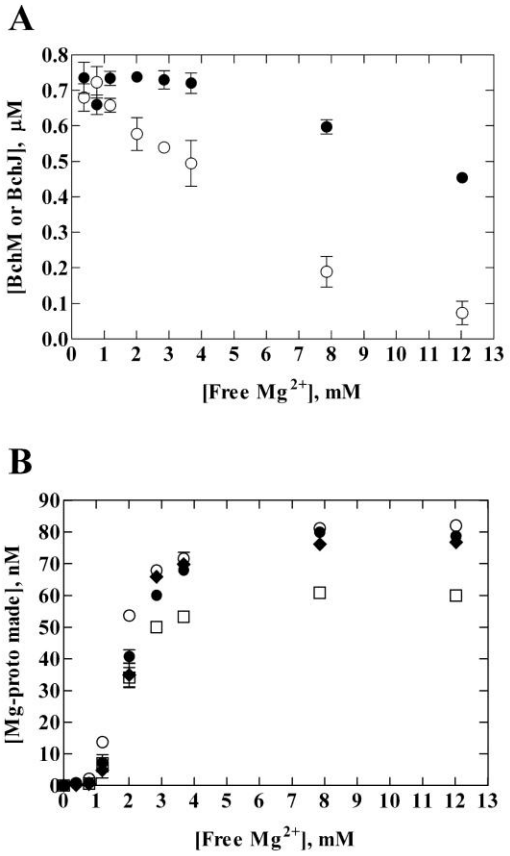

Figure 2
118x176mm (600 x 600 DPI)

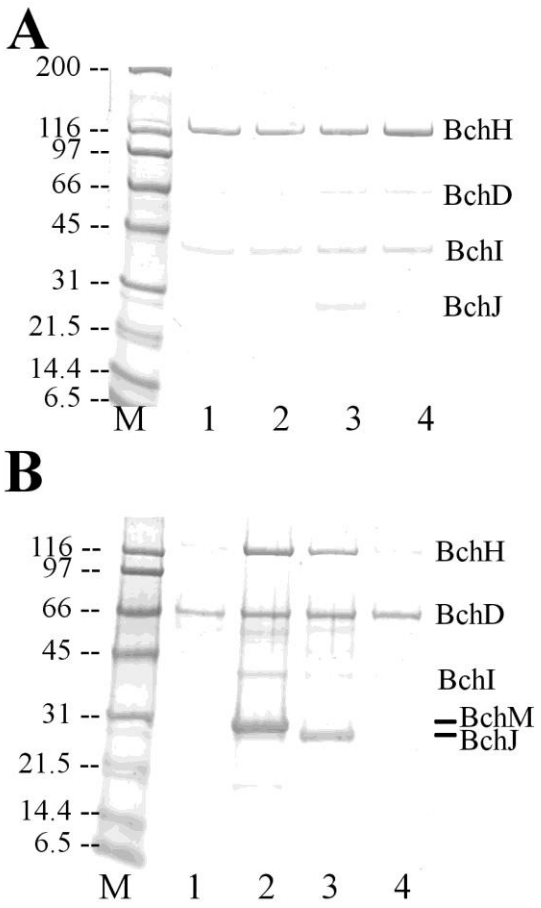

Figure 3
77x126mm (300 x 300 DPI)

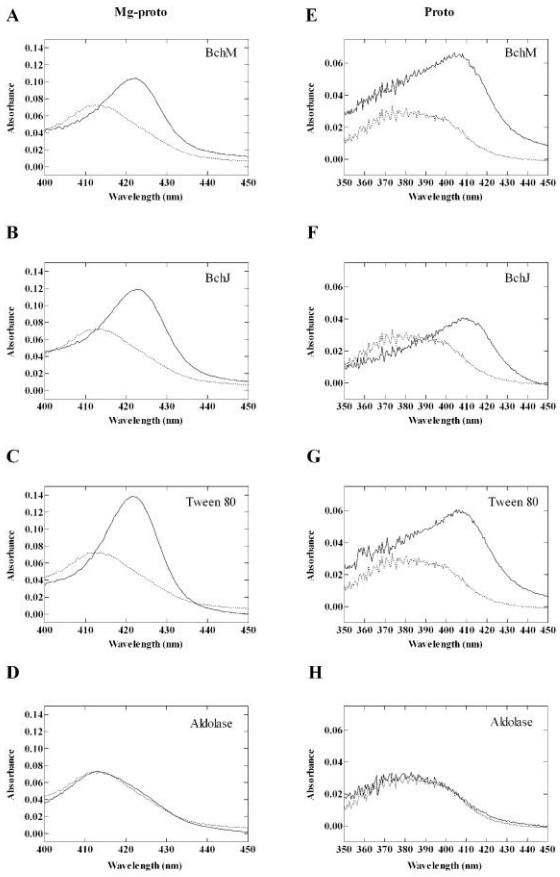

Figure 4
159x236mm (600 x 600 DPI)

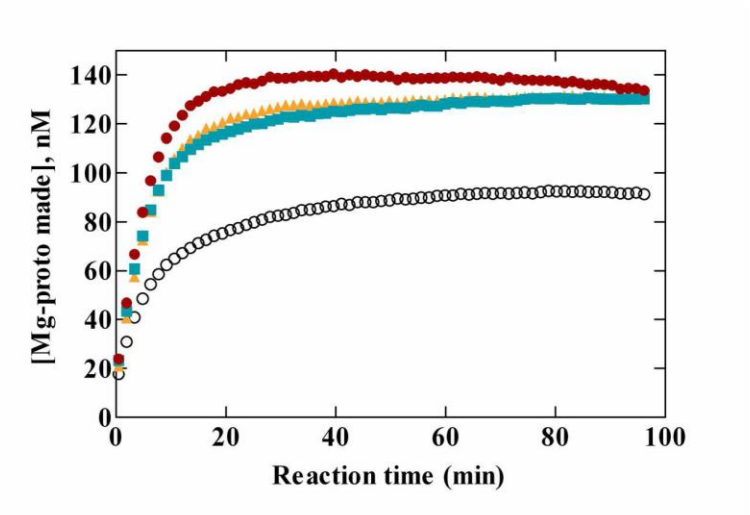

Figure 5
54x36mm (600 x 600 DPI)

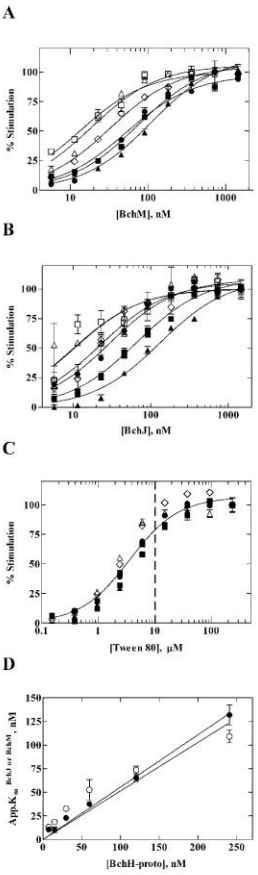

Figure 6
79x227mm (1200 x 1200 DPI)

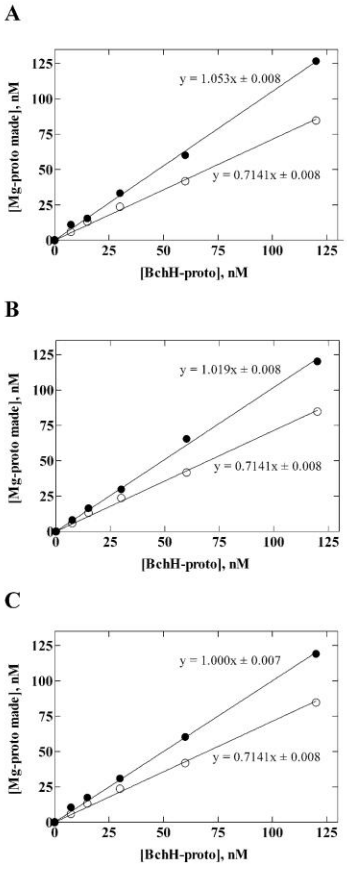

Figure 7
172x374mm (600 x 600 DPI)

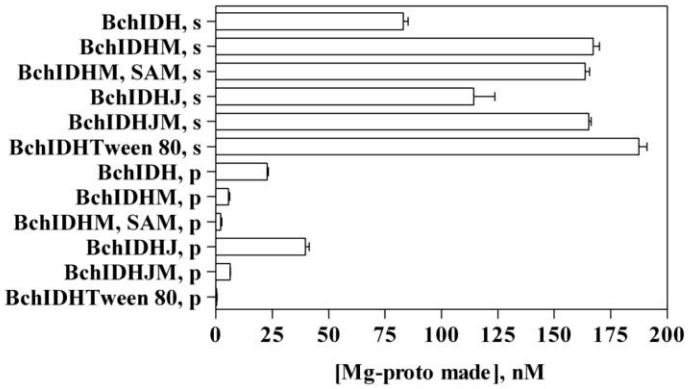

Figure 8
47x27mm (600 x 600 DPI)

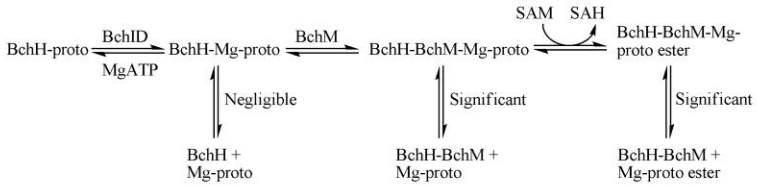

Schematic 1
185x45mm (300 x 300 DPI)

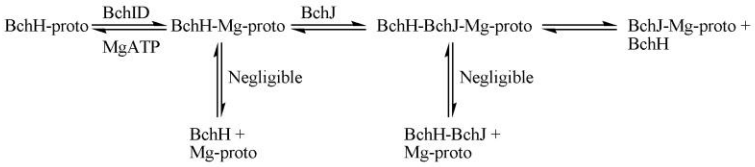

Schematic 2
180x39mm (300 x 300 DPI)

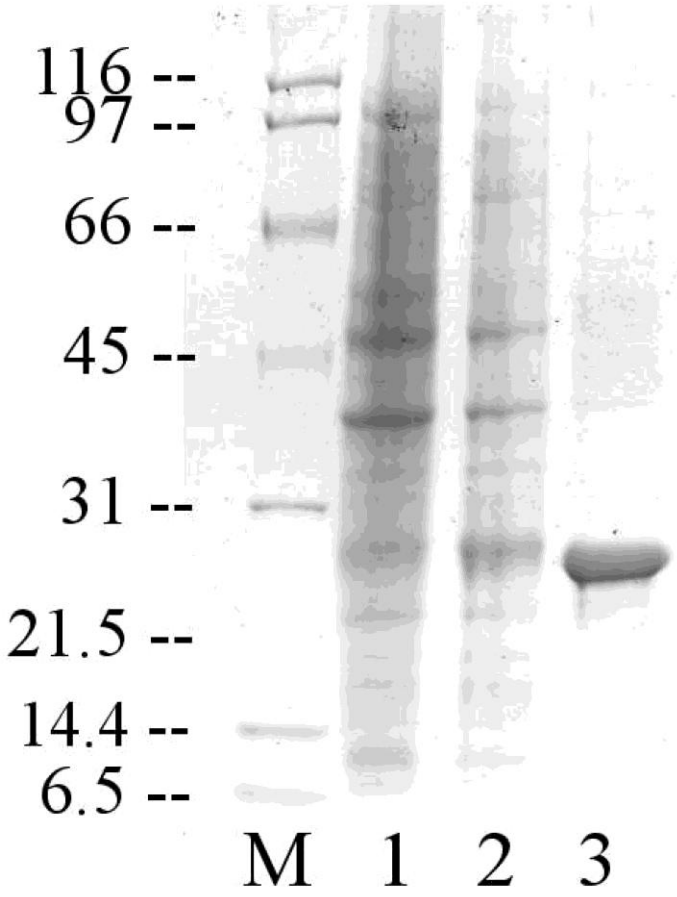

Supplementary Figure 1
39x51mm (300 x 300 DPI)

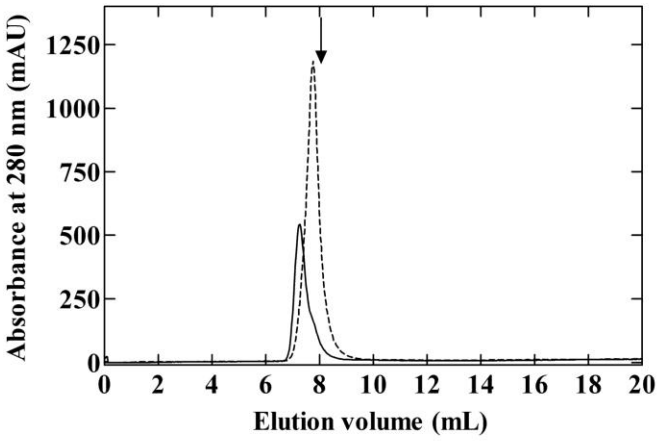

Supplementary Figure 2
65x44mm (600 x 600 DPI)

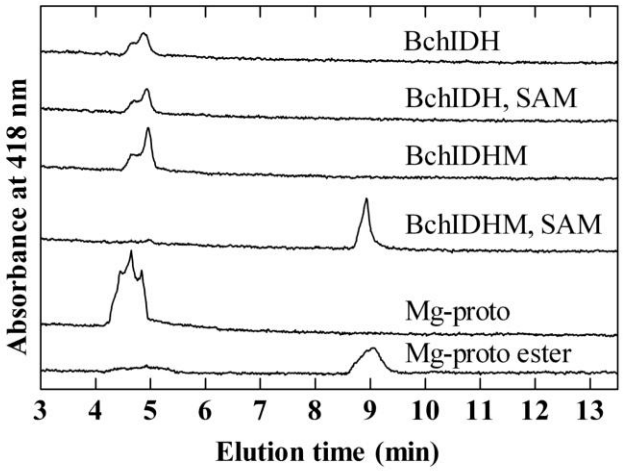

Supplementary Figure 3
66x44mm (600 x 600 DPI)